A Novel Large Animal Model of Smoke Inhalation-Induced Acute Respiratory Distress Syndrome

Premila Leiphrakpam
University of Nebraska Medical Center
Hannah Weber
University of Nebraska Medical Center
Andrea McCain
University of Nebraska-Lincoln
Roser Romaguera Matas
University of Nebraska-Lincoln
Ernesto Martinez Duarte
University of Nebraska Medical Center
Keely Buesing (keely.buesing@unmc.edu)
University of Nebraska Medical Center https://orcid.org/0000-0002-8461-1938

Research

Keywords: Smoke inhalation, ARDS, large animal model, toxic inhalation injury, hypoxia, hypoxemia

Posted Date: March 13th, 2021

DOI: https://doi.org/10.21203/rs.3.rs-297210/v1

Version of Record: A version of this preprint was published at Respiratory Research on July 7th, 2021. See the published version at https://doi.org/10.1186/s12931-021-01788-8.

Abstract

Background

Acute respiratory distress syndrome (ARDS) is multifactorial and can result from sepsis, trauma, or pneumonia, amongst other primary pathologies. It is one of the major causes of death in critically ill patients with a reported mortality rate up to 45%. The present study focuses on the development of a large animal model of smoke inhalation-induced ARDS in an effort to provide the scientific community with a reliable, reproducible large animal model of isolated toxic inhalation injury-induced ARDS.

Methods

Animals (n = 21) were exposed to smoke under general anesthesia for 1 to 2 hours (median smoke exposure = 0.5 to 1 liter of oak wood smoke) after the ultrasound-guided placement of carotid, pulmonary, and femoral artery catheters. Peripheral oxygen saturation (SpO_2), vital signs, and ventilator parameters were monitored throughout the procedure. Chest x-ray, carotid, femoral and pulmonary artery blood samples were collected before, during, and after smoke exposure. Animals were euthanized and lung tissue collected for analysis 48 hours after smoke inhalation.

Results

Animals developed ARDS 48 hours after smoke inhalation as reflected by a decrease in SpO_2 by approximately 31%, PaO_2/FiO_2 ratio by approximately 208, and development of bilateral, diffuse infiltrates on chest x-ray. Study animals also demonstrated a significant increase in IL-6 level, lung tissue injury score and wet/dry ratio, as well as changes in other arterial blood gas (ABG) parameters.

Conclusions

This study reports, for the first time, a novel large animal model of isolated smoke inhalation-induced ARDS without confounding variables such as cutaneous burn injury. Use of this unique model may be of benefit in studying the pathophysiology of inhalation injury or for development of novel therapeutics.

Introduction

Acute respiratory distress syndrome (ARDS) is a lethal disease condition in critically ill patients with a reported mortality rate ranging from 30–45% [1, 2]. There has been no significant change in the mortality rate since 1994 [2]. ARDS can be caused by a variety of direct and indirect injuries to the lung, including sepsis, trauma, pneumonia and smoke inhalation/burn injury [3–5]. Understanding the

pathophysiological and molecular mechanisms of ARDS is critical for the development of novel therapeutic strategies for ARDS.

ARDS was coined by Ashbaugh *et al.* in 1967 to describe an acute onset of tachypnea, hypoxemia, and loss of compliance after a variety of insults [6]. The most current consensus definition for ARDS in clinical setting was published in 2012 as the Berlin criteria [7]. The Berlin criteria base categorization of ARDS on level of hypoxemia measured by the PaO_2/FiO_2 (arterial oxygen partial pressure / fraction of inspired oxygen) ratio, positive end-expiratory pressure (PEEP) level, development of bilateral pulmonary infiltrates on chest x-ray, and normal pulmonary capillary wedge pressure (PCWP) within a week of a known clinical insult [7]. The lung injury in ARDS has been reported to undergo three pathophysiological phases: the exudative phase involves damage to the alveolar epithelium leading to increased lung permeability; the proliferative phase involves type II cell proliferation with epithelial cell regeneration, fibroblastic reaction, and remodeling; and the irreversible fibrotic phase, which includes collagen deposition in the lung [8–10]. To understand the development of ARDS, reliable animal models that can mimic these pathophysiological phases are critical. Previous studies have used mouse models for assessment of pulmonary gas exchange and respiratory physiology following controlled induction of ARDS [11, 12]. However, these mouse models have limitations in the induction of mechanical ventilation and collection of blood samples, and are therefore, not amenable for prolonged study essential to mimic the clinical presentations of ARDS. Large animal models have been reported to show better translational potential in the study of ARDS. Swine models are considered an excellent model for pulmonary pathology due to the similarities with humans in terms of anatomy, genetics and physiology [13]. Various studies have used swine models to study lung development [14, 15], acute lung injury (ALI)/ARDS [16, 17] and other diseases.

Smoke inhalation is one of the major causes for the development of ARDS after burn injury, with an approximate 30%-90% mortality rate [18, 19]. Several large animal models are available for smoke/burn injury-induced ARDS [17, 20–22]. However, at present, there is no suitable large animal model available to study isolated smoke inhalation-induced ARDS without confounding variables such as cutaneous burn injury.

We have developed a large animal, isolated smoke inhalation model to use in our investigations of molecular modification after smoke inhalation and novel therapeutic agents. In the study, pigs were exposed to smoke directly through an endotracheal route to induce lung injury in a controlled environment. Invasive and non-invasive parameters including vital signs, arterial blood gas analysis, and chest x-rays were monitored to pinpoint the development of significant ARDS. Cytokine and histological analysis was performed to understand the pathophysiological profile critical for the development of ARDS in these animals. To our knowledge, this is the first study to develop and detail a large animal model of isolated smoke inhalation-induced ARDS.

Methods

Subjects

All the experiments involving animals were approved by University of Nebraska Lincoln (UNL) Institutional Animal Care and Use Committee (IACUC) (protocol # 1674).
Female pigs (~ 50 kg, n = 21) were housed in Animal Science Complex, UNL in experimental pens and cared for according to USDA (United States Department of Agriculture) guidelines. Animals were acclimated to the facility for 4–7 days and received food reward training to ease handling and blood draws. Six animals died during the experiments due to either anesthesia/surgical complications or smoke inhalation related complication. We continued our next phase of study (involving efficacy of a novel therapeutic for hypoxia) in some of these animals to reduce cost and number of animals used.

Smoke Delivery System

Upon completion of all surgical procedures, animals were exposed to oak wood smoke from a custom-made smoke generator connected in parallel to the endotracheal tube. Schematic is shown in Fig. 1.

Surgical Procedures

Sedation for peripheral intravenous catheter (PIV) placement and endotracheal intubation was achieved with a mixture of telazol (4.4 mg/kg), ketamine (2.2 mg/kg) and xylazine (2.2 mg/kg) delivered via intramuscular injection. To assist with intubation, an intravenous bolus dose of fentanyl (0.05 mg/kg) and/or propofol (2-4.4 mg/kg) was given as needed. Baseline chest x-rays were obtained (portable x-ray unit EPX-F2800, Ecotron Co. Ltc; wireless digital flat panel detector Mars1417V-TSI, iRay Technology, Shanghai, China) prior to smoke inhalation, and at 24 and 48 hours after smoke inhalation. An endotracheal tube (#7–8 cuffed; MWI Animal Health, Boise, ID, USA) was inserted into the trachea and animals were ventilated at a tidal volume (TV) of 6 mL/kg and peak end expiratory pressure (PEEP) of 5 cmH_2O (Newport HT70, Medtronic, Minneapolis, MN). Respiratory rate (RR) was adjusted to maintain eucapnia as monitored by end-tidal CO_2 ($ETCO_2$). The fraction of inspired oxygen (FiO_2) was set at 50% during surgical procedures (central venous & arterial catheter placement), then titrated down to 21% and maintained throughout the experiment. Non-invasive monitoring included blood pressure taken by cuff placed around the animal's hind leg, peripheral oxygen saturation (SpO_2), heart rate (HR) and $ETCO_2$ recorded via the Surgivet monitor (Smiths Medical, Dublin, OH). Continuous IV sedation containing midazolam (0.4–0.7 mg/kg/h), fentanyl (0.03–0.1 mg/kg/h) and propofol (0.2–0.4 mg/kg/min) and maintenance IV fluids (10 mL/kg/h normal saline) were given throughout the procedure via a quadruple-lumen central venous catheter (8.5Fr x 16 cm, Arrow International) placed in the internal jugular vein. Core temperature was monitored by rectal probe and a circulating warming blanket was used to prevent body cooling. A urinary catheter was placed to monitor output.

Using sterile technique and ultrasound guidance (Butterfly iQ, Butterfly Network, New York City, NY), carotid artery (CA) and femoral artery (FA) access catheters were placed for serial lab draws and invasive blood pressure monitoring (18 GA 16 cm; Femoral Arterial Line Catherization Kit; Teleflex, Morrisville, NC).

Pulmonary artery (PA) catheter (8F x 110 cm Swan-Ganz CCOmbo Thermodilution Catheter; Edwards Lifesciences, Irvine, CA) was placed in the internal jugular vein under ultrasound guidance. The CA and PA access ports were connected to Surgivet monitor and Vigilance II monitor, respectively (Edwards Lifesciences, Irvine, CA) with transducers (Meritans DTXPlus, Disposable Pressure Transducer with EasyVent; Merit Medical, South Jordan, UT, USA). Invasive arterial blood pressure, central venous pressure (CVP), pulmonary artery pressure (PAP), cardiac output (CO), mixed venous oxygen saturation ($SmvO_2$), and central (core) temperature were monitored throughout the study. Blood samples were drawn from the CA, FA and PA catheters for the measurement of baseline blood gas prior to smoke inhalation and at pre-determined time intervals throughout the study period (ABL80 FLEX CO-OX, Radiometer, Brea, CA). To maintain patency, catheters were flushed throughout the experiment with 3–5 mL of sterile saline, and a heparin solution (1:500 dilution in 50% dextrose solution) was infused to fill the volume of the port chosen as a "lock" solution. Sedated/anesthetized animals from survival surgeries were continuously monitored until sternal recumbence was regained. All catheters were removed after smoke inhalation was completed. The surgical procedures were repeated at 48 h after smoke inhalation.

Smoke Inhalation

Upon completion of surgical procedures, animals in the SI group were exposed to oak wood smoke from the custom-made smoke chamber (Fig. 2) through the endotracheal tube. The duration of the smoke exposure was 1 to 2 hours starting from 0h time point. The volume of smoke inhaled was approximately 500 liters per hour. Invasive and noninvasive parameters were monitored continuously during the experiment. Following smoke exposure, blood samples were collected from arterial ports and PAC. Animal was continuously monitored until recovery from general anesthesia. Smoke exposure was stopped immediately if the animal developed hemodynamic instability, which was determined by hypotension (systolic blood pressure less than 60) and irreversible desaturation (SpO_2 less than 70% despite rescue maneuvers such as increase in inspired percentage of oxygen).

Ventilator Parameters

On the day of the smoke inhalation, the ventilator parameters were maintained at values: tidal volume, 6 mL/kg = 270-360L/min; respiratory rate, 18–30/min; PEEP 5mmHg; and FiO_2, 21–34% (Table 2). During the 48h after smoke inhalation surgery, animals were extubated and maintained on room air.

Table 2
Ventilator parameters

Parameters	Baseline	2h	24h	48h
TV (mL/kg)	270–360	270–360	--	220–280
RR (bpm)	18–30	18–30	--	16–24
FiO_2(%)	21–34	21–34	21	21
PEEP (cmH2O)	5	5	---	0

TV, tidal volume; RR, respiratory rate; bpm, beats per minute; FiO_2, fraction of inspired oxygen; PEEP, positive end expiratory pressure; n = 13.

Post-Surgical Animal Monitoring and Care

After recovery from surgical anesthesia, all animals were transferred to the post-surgery recovery pen and were monitored 24h/day by trained personnel. Chest x-rays were taken and blood samples drawn for ABG analysis at 24h and 48h following final smoke exposure. Animals (n = 7) were humanely euthanized at 48h post SI and a full necropsy was performed; the remainder of animals were utilized to continue our lab's therapeutic investigations.

Plasma Sample Extraction

Blood samples were collected from the CA catheter at baseline, 2h, and 48h time points in lithium heparin BD Microtainer tubes (Becton, Dickinson and Company, Franklin Lakes, NJ). Tubes were immediately inverted 8–10 times to assure anticoagulation and centrifuged at 8000 g for 4 minutes. Supernatants were collected as plasma samples and stored at -20 ºC until analysis. IL-6 immune assay was performed in samples of 10 animals using IL-6 Quantikine® ELISA kit, catalog No#P6000B (R&D Systems, Inc., Minneapolis, MN) on plasma samples following manufacturer's protocol.

Bronchoalveolar Lavage (BAL)

BAL of pig lungs was performed at baseline, 2h, and 48h time points using a bronchoscope in a set of 6 intubated animals. 10 ml of sterile normal saline was instilled to the secondary and tertiary bronchi through the bronchoscope and ~ 5ml of the fluid was collected for analysis. BAL fluid samples were centrifuged immediately at 4000 g at 4°C for 10 minutes and supernatants were at stored at -20 ºC until analysis. Total protein quantification was performed in samples using Pierce™ BCA (Bicinchoninic Acid) Protein Assay Kit (Thermo Fisher Scientific Inc. Waltham, MA) following manufacturer's protocol. IL-6 immune assay was performed using IL-6 Quantikine® ELISA (Enzyme-linked immunosorbent assay) kit, catalog No#P6000B (R&D Systems, Inc., Minneapolis, MN) on BAL fluid samples following manufacturer's protocol.

Tissue Collection

Necropsy was performed in 7 animals. At necropsy, lung tissues were collected from all five lobes; upper, middle and lower lobes of right lung and upper and lower lobes of left lung for histological examination and pulmonary edema assessment. Tissues for histology were immediately placed in 10% neutral buffer formalin fixative for approximately 24 hours. Formalin fixed tissues were placed into 70% ethanol and transferred to the University of Nebraska Medical Center (UNMC) Tissue Science Facility (TSF) for further tissue processing and embedment in paraffin blocks.

Lung Injury Score

The lung tissue in 10% neutral formalin was dehydrated in graded concentrations of ethanol solution and cleared in xylene. The tissue samples were then paraffin-embedded, sectioned with 4-µm thickness, and stained with hematoxylin and eosin at the UNMC Tissue Sciences Facility using automated Ventana Discovery Ultra (Roche Diagnostics, Indianapolis, IN) as per manufacturer's protocol. An independent pathologist performed a blinded examination of the tissues under light microscope. Ten fields of each lung tissue section were examined at magnification x400. The severity of the lung injury was scored by the criteria of alveolar edema, intra-alveolar hemorrhage, and leukocyte infiltration. Alveolar edema and intra-alveolar hemorrhage were scored on a scale from 0 to 3; where 0 = < 5% of maximum pathology, 1 = mild (< 10%), 2 = moderate (10–20%), and 3 = severe (20–30%). Leukocyte infiltration was also scored on a scale from 0 to 3; where 0 = absence of extravascular leukocytes, 1 = < 10, 2 = 10–45, and 3 = > 45 leukocytes.

Wet-to-dry weight (W/D) ratio

Lung tissues (n = 6) were dried in an incubator at 60°C for 5 days and weighed again (dry weight). The W/D ratio was calculated as the ratio of the wet weight to the final dry weight as described elsewhere [23].

Ki67 Immunohistochemistry

Immunostaining for Ki67 was performed on pig SI and control formalin-fixed, paraffin-embedded lung tissues sections at UNMC Tissue Sciences Facility using automated Ventana Discovery Ultra (Roche Diagnostics, Indianapolis, IN) in lung tissue samples of 4 animals as per manufacturer's protocol. Specimens were processed on the same day to eliminate any variability in conditions. An independent pathologist performed a double-blinded examination of the tissue slides under a light microscope. A total of 2000 cells were counted at magnification of X400 and the percentage of Ki67 positive cells were calculated.

Lung Tissue Lysate Preparation

Fresh frozen lung lobe tissues with highest injury score (n = 5) were homogenized using VWR® Mini Bead Mill Homogenizer (VWR International LLC., Radnor, PA) following manufacturer's protocol. Briefly, frozen tissues of two control and three SI animals were washed in cold X1 PBS, and 30 mg of each tissue was placed separately in a 2 mL tube containing 2.8 mm ceramic beads and 750 µl of lysis buffer containing RIPA buffer (Thermo Fisher Scientific Inc. Waltham, MA) and protease inhibitor cocktail (Sigma Aldrich

Inc., St. Louis, MO) at room temperature. The samples were homogenized at speed 4 for 60 seconds. This was followed by incubation in ice for 30 minutes and centrifugation at 13,000 rpm for 20 minutes at 4 ºC. Protein concentration was determined using Pierce™ BCA (Bicinchoninic Acid) Protein Assay Kit (Thermo Fisher Scientific Inc. Waltham, MA) following manufacturer's protocol.

Immunoblot Analysis

Protein (50 µg) was separated by SDS- polyacrylamide gel electrophoresis and transferred onto PVDF (polyvinylidene fluoride) membrane (Bio-Rad Lab Inc., Hercules, CA) by electro blotting. The membrane was blocked with 5% nonfat dry milk in X1 TBST (50mM Tris, pH 7.5, 150mM NaCl, 0.01% Tween 20) for 1 hour at room temperature. The membrane was then incubated in primary antibody, IL-6 antibody (#ab6672, Abcam Inc, Cambridge, MA) or β-actin (#4970, Cell Signaling Technology Inc., Danvers, MA) at 1:1000 dilution in X1 TBST with 5% bovine serum albumin (Sigma Aldrich Inc., St. Louis, MO) overnight at 4°C. The membrane was washed three times with X1 TBST for 10 minutes each and incubated with HRP-conjugated secondary antibody (#7074, Cell Signaling Technology Inc., Danvers, MA) at 1:5000 dilution in X1 TBST with 5% nonfat dry milk for 1 hour at room temperature. Following washes in X1 TBST, proteins were detected using the enhanced chemiluminescence system (Bio-Rad Lab Inc, Hercules, CA).

Statistical Analysis

Statistical analysis was performed using GraphPad prism 8. One-way ANOVA with Tukey's post-hoc analysis and paired t test were utilized to generate adjusted "p" values. P-values < 0.05 were considered statistically significant.

Results

The study was divided in two phases. The first phase of the study was performed to determine the optimal duration of smoke exposure required for the development of ARDS. Animals were divided according to smoke inhalation time as shown in the flow diagram in Fig. 2. Smoke inhalation for 1 h was designated as "SI 1h" (n = 3) and smoke inhalation for 2 h was designated as "SI 2h" (n = 18). Fifteen animals successfully completed smoke inhalation (SI) experiment and survived 48h post smoke exposure, and six animals died during procedures due to either anesthesia/surgical complications or smoke inhalation-related complication.

Smoke inhalation reduced peripheral oxygenation in large animal model

The SpO_2 level was measured continuously on the day of the smoke inhalation experiment and at 24h- and 48h- post smoke inhalation. The SpO_2 level following 1h- or 2h- smoke inhalation was approximately 95% and started to decrease at 24h post smoke inhalation in both groups. However, SpO_2 level significantly dropped in the SI 2h group at 48h post smoke exposure (68 ± 6 %) compared to baseline (98 ± 2 %) and the SI 1h group (88 ± 4%) (Fig. 3A). The decrease was approximately 30% as reflected by the

delta SpO_2 (ΔSpO_2) value in SI 2h group compared 10% in the SI 1h group (Fig. 3B). In addition, at 48h post smoke exposure PaO_2/FiO_2 ratio was reduced approximately to 193.4 in the SI 2h group compared to baseline and SI 1h group values (267–390) (Figs. 3C and 3D). These results demonstrated that smoke inhalation for 2h induced significant injury to the lung at 48h post smoke exposure.

For the rest of the study, we concentrated at the 2h time point for duration of smoke exposure, and repeated experiments to ensure reproducibility of this model. Animals were exposed to smoke for 2h duration and designated as “SI” animals. Consistent with the result in Fig. 3, we observed a 22–40% decrease in SpO_2 compared to baseline values (Figs. 4A and 4B, $p < 0.0001$). In addition, arterial and mixed venous oxygen saturation (SaO_2 and $SmvO_2$) were reduced by approximately 39–43% compared to the corresponding baseline values (Figs. 4C and 4D, $p < 0.0001$).

All results presented to follow are after 2h smoke exposure.

Smoke inhalation induced hypoxemia in large animal model

Arterial blood gas (ABG) was measured from both arterial and mixed venous blood samples throughout the study. The arterial partial pressure of oxygen (PaO_2) level started to decrease 1h after smoke exposure and dropped significantly at 48h post smoke exposure to 43 mmHg from baseline value of 95 mmHg (Fig. 5A). Delta PaO_2 (ΔPaO_2) value in Fig. 5B showed a difference of 53 ± 5.8 mmHg ($p < 0.0001$). As expected, there was a rise in partial pressure of carbon dioxide ($PaCO_2$) level (Fig. 5A) with an increase in $\Delta PaCO_2$ value by 27.5 ± 2.34 mmHg compared to the baseline value (Fig. 5B, $p < 0.0001$). In correlation with findings from arterial samples, at 48h post smoke exposure we observed significant reduction in the partial pressure of mixed venous oxygen ($\Delta PmvO_2$) level (15.12 ± 2.12 mmHg) and corresponding increase in partial pressure of mixed venous carbon dioxide ($\Delta PmvCO_2$) level (19.23 ± 4.01 mmHg) compared to the baseline values (Figs. 5C and 5D, $p < 0.0001$ to $= 0.0005$). The pH level was also significantly decreased at 48h post smoke inhalation (Table 1, $p < 0.001$) with no significant change in the HCO_3 levels (Table 1). Consistent with the rise in $PaCO_2$ value post smoke inhalation, end tidal CO_2 ($ETCO_2$) – which measures the concentration of CO_2 exhaled at the endotracheal tube – significantly increased from the baseline value of 33.9 ± 12.8 mmHg to 52.63 ± 13.5 mmHg at 48 h post smoke inhalation (Table 1, $p = 0.009$).

Table 1
Hemodynamic parameters

Parameters	Baseline	2h	24h^	48h
Art pH	7.47 ± 0.07	7.45 ± 0.07	7.47 ± 0.04	7.30 ± 0.10***
Art HCO_3 (mmol/L)	29.33 ± 2.19	30.42 ± 1.80	27.49 ± 3.02	30.09 ± 3.70
$ETCO_2$ (mmHg)	33.90 ± 12.8	40.56 ± 11.8	—	52.63 ± 13.5**
Hct (%)	34.35 ± 2.82	34.02 ± 3.46	31.75 ± 2.99	29.58 ± 6.04*
Hb (g/dl)	11.08 ± 0.84	11.04 ± 1.15	10.37 ± 0.94	9.50 ± 1.89*
FO_2Hb (%)	95.35 ± 3.80	91.74 ± 7.89	—	52.13 ± 16.4***
HR (bpm)	87.17 ± 18.3	92.91 ± 41.63	—	88.75 ± 12.88
Temp (ºC)	37.18 ± 0.87	36.67 ± 4.43	—	41.27 ± 11.1
MAP (mmHg)	66.50 ± 26.8	72.68 ± 12.8	—	74.83 ± 19.0
PAP (mmHg)	15.25 ± 9.20	14.71 ± 10.2	—	23.84 ± 17.2

Values are mean ± SD, n = 13. Art pH, arterial pH; Art HCO_3, arterial bicarbonate; $ETCO_2$, end tidal carbon dioxide; Hct, hematocrit; Hb, hemoglobin; FO_2Hb, fractional oxyhemoglobin MAP, mean arterial pressure; PAP, pulmonary arterial pressure; HR, heart rate; Temp, temperature. **p < 0.01, ***p < 0.001, ****p < 0.0001

^ n = 8

Previous studies have documented PaO_2/FiO_2 ratio to assess the level of hypoxemia in the animal model [17, 24]. We also demonstrated significant reduction in PaO_2/FiO_2 ratio at 48h post smoke exposure (198.87 ± 37.13), with 40% of animals having values less than 170 (Fig. 6A). The difference in the $\Delta PaO_2/FiO_2$ value between the baseline and at 48h post smoke exposure was approximately 208 (Fig. 6B, p < 0.0001). Furthermore, hematocrit (Hct), hemoglobin (Hb), and fractional oxyhemoglobin (FO_2Hb) values were reduced 48h after smoke inhalation compared to baseline (Table 1, p < 0.001 to = 0.02). As expected, total arterial oxygen content (CaO_2) and mixed venous oxygen content ($CmvO_2$) of blood were also significantly reduced 48h after smoke inhalation compared to the corresponding baseline values (Figs. 6C and 6D, p < 0.0001). There were no significant changes in heart rate (HR), temperature (Temp), mean arterial pressure (MAP) and pulmonary arterial pressure (PAP) (Table 1).

Effect of smoke inhalation on lung parenchyma

Smoke inhalation has been reported to increase capillary leakage [25–27]. Consistent with previous studies, we observed diffuse, bilateral infiltrates on repeated radiographic assessment of lung injury with chest x-rays in both ventral-dorsal and lateral views at 48h after smoke injury (Fig. 7A). In contrast, both lungs were normal in the chest x-rays taken before smoke inhalation (Fig. 7A). Histologic examination of

lung tissue 48h post smoke exposure showed an increase in the number of leukocyte infiltration, intra-alveolar hemorrhage, and alveolar edema compared to the control animal group (Figs. 7B and 7C); and the overall lung injury score was significantly increased (Fig. 7D; $p = 0.0001$). We also observed an increase in the average wet-dry weight (W/D) ratio of lung tissues 48h after smoke exposure (6.233 ± 1.14) compared to the control animals (5.445 ± 0.36) (Fig. 7E, $p = 0.0091$). Ki67 immunohistochemistry was performed in paraffin embedded lung tissue sections of two control and two smoke inhalation animals. Lung tissue sections of animals at 48h post smoke inhalation showed a statistically significant decrease in the number of proliferative cells compared to the control animals (Fig. 7F, $p = 0.0498$). Furthermore, BAL fluid samples taken from six animals showed significant increase in the total protein concentration of BAL fluid 48h post smoke inhalation compared to the baseline (Fig. 7G, $p = 0.0436$).

Effect of smoke inhalation on IL-6 expression level

We observed a significant increase in IL-6 level in BAL fluid samples at 48h post smoke exposure (Fig. 8A, $p = 0.0102$), and a marginal increase at 2h time point (Fig. 8A, $p = 0.1010$) compared to the baseline level. IL-6 immune assay analysis in plasma samples of 10 animals also demonstrated a significant increase in IL-6 level in SI animals at 2h smoke inhalation compared to the baseline (Fig. 8B, $p = 0.0046$). However, no significant increase was observed in animals at 48h post smoke inhalation (Fig. 8B, $p = 0.1934$). Increased IL-6 expression level obtained in BAL fluid and plasma sample immunoassay analyses were further validated by the robust upregulation of IL-6 expression level in immunoblotting at 48h post smoke inhalation in SI animals compared to the control animals (Fig. 8C).

Discussion

ARDS arises from diverse insults in the lungs, and a variety of lung injury animal models have been developed to study the pathophysiological processes [3, 28]. Frequently used models for ALI includes intravenous infusion of oleic acid [29, 30], repeated bronchoalveolar lavage with saline [31, 32], and intravenous infusion of endotoxin [33, 34]. These models studied acute lung injury manifested within 24 hours. However, these models were not closely related to the clinical situation in ARDS [35]. Therefore, a chronic animal model of lung injury after insults would better represent the clinical manifestation of ARDS and may help in the development of novel therapeutic strategies.

Furthermore, no large animal models of ARDS from isolated smoke inhalation injury exists in the literature. Our main goal was to contribute to the scientific community by developing such a model that is reliable and reproducible. Smoke inhalation is a major predisposing factor for the development of ARDS and is considered together with burn injury in several animal models for smoke/burn injury-induced ARDS [17, 20–22]. However, there is no suitable large animal model available for isolated smoke inhalation-induced ARDS that replicates human ARDS without confounding variables such as cutaneous burn injury.

In the present study, we reported the development and validation of a large animal model for isolated smoke inhalation-induced ARDS. Following smoke exposure through an endotracheal tube, animal

reproduced the entire set of clinical parameters for defining ARDS, such as significant decrease in SpO_2 to approximately 65%, mean PaO_2/FiO_2 value of 196, diffuse bilateral pulmonary infiltrates on chest X-rays at 48h post smoke inhalation, and no clinical evidence of cardiac failure or fluid overload as explained by ARDS Definition Task Force, 2012 [7]. We also documented significant decreases in PaO_2 and the reciprocal increase in $PaCO_2$. Studies have shown that increases in $PaCO_2$ and $ETCO_2$ levels correlate with the presence of physiological dead space in lungs and the increased in gradient between these two values corresponds with ARDS severity [36, 37]. We observed an increase in the gradient ($PaCO_2$ - $ETCO_2$) from 7.67 at baseline to 14.21 at 48 h post smoke exposure. IL-6, one of the inflammatory cytokines involved in the development of ARDS started to rise 2h time point in SI animals and sustained until 48h in both plasma and BAL fluid samples. IL-6 expression level was also significantly upregulated in fresh frozen lung tissue samples of smoke exposed animals compared to control animals. In addition, evidence of significant lung tissue injury and inflammatory response to the injury were documented. These results indicated the deterioration of respiratory functions in the diseased lungs from smoke exposure.

Developing mimics of human ARDS in a large animal model such as pig has clear advantages, such as the ability to perform invasive procedures and serial blood analysis, and feasibility of documenting the respiratory function for an extended period of time. Moreover, monitoring the respiratory parameters in a mechanically ventilated animal allowed us to detail functional deterioration of the animal in a controlled environment after smoke inhalation. The detailed presentation of our model allows for others in the scientific community to independently confirm reproducibility, and hopefully use our model for investigations leading to clinical translation.

Conclusion

We developed, for the first time, a novel large animal isolated smoke inhalation-induced ARDS model which mimics human ARDS and lacks confounding variables such as cutaneous burn injury or intra-abdominal sepsis. This model will help in better understanding the pathophysiological mechanisms involved in the process of smoke inhalation-induced ARDS and aid in the development of novel therapeutic strategies.

Abbreviations

ABG
Arterial blood gas
ALI
Acute lung injury
ANOVA
Analysis of variance
ARDS

Acute respiratory distress syndrome
BAL
Bronchoalveolar lavage
BCA
Bicinchoninic Acid
CaO_2
Arterial oxygen content
$CmvO_2$
Mixed venous oxygen content
CA
Carotid artery
CO
Cardiac output
CVP
Central venous pressure
ELISA
Enzyme-linked immunosorbent assay
$ETCO_2$
End-tidal carbon dioxide
FA
Femoral artery
FiO_2
Fraction of inspired oxygen
HCO_3
Hydrogen bicarbonate
HR
Heart rate
IL-6
Interleukin-6
MAP
mean arterial pressure
PA
Pulmonary artery
PAP
Pulmonary artery pressure
$PaCO_2$
Partial pressure of carbon dioxide
PaO_2
Arterial oxygen partial pressure

PCWP
Pulmonary capillary wedge pressure
PEEP
Positive end-expiratory pressure
PIV
Peripheral intravenous catheter
$PmvO_2$
Partial pressure of mixed venous oxygen
PVDF
Polyvinylidene fluoride
RR
Respiratory rate
$SmvO_2$
Mixed venous oxygen saturation
SpO_2
Peripheral oxygen saturation
TBST
Tris-Buffered Saline, 0.1% Tween® 20 Detergent
TV
Tidal volume
W/D
Wet-to-dry weight

Declarations

ETHICS APPROVALAND CONSENT TO PARTICIPATE: All the experiments involving animals were approved by University of Nebraska Lincoln (UNL) Institutional Animal Care and Use Committee (IACUC) (protocol # 1674).

CONSENT FOR PUBLICATION: NA

AVAILABILITY OF DATA AND MATERIALS: Data are available upon reasonable request from the corresponding author.

COMPETING INTERESTS: The authors declare no competing or financial interests.

FUNDING: The study was financially supported by award FA4600-12-D-9000 from the Department of Defense U.S. Air Force.

AUTHOR CONTRIBUTIONS: Conceived and designed the study: K.L.B. Acquired, analyzed and interpret data: K.L.B., P.D.L., H.R.W. Performed histological analysis: E.M.D. Performed experiment with mechanically ventilated pig: K.L.B., P.D.L., H.R.W., A.M., R.R.M. Wrote manuscript: K.L.B., P.D.L. All authors read and approved the manuscript prior to submission.

ACKNOWLEDGEMENTS: We would like to thank the Institutional Animal Care staff at UNL for the help during the surgical procedures and for monitoring the animals included in this study.

References

1. Máca J, Jor O, Holub M, Sklienka P, Burša F, Burda M, et al. Past and Present ARDS Mortality Rates: A Systematic Review. Respiratory Care. 2017;62(1):113-122.
2. Phua J, Badia JR, Adhikari NKJ, Friedrich JO, Fowler RA, Singh JM, et al. Has Mortality from Acute Respiratory Distress Syndrome Decreased over Time? American Journal of Respiratory and Critical Care Medicine. 2009;179(3):220-227.
3. Bakowitz M, Bruns B, McCunn M. Acute lung injury and the acute respiratory distress syndrome in the injured patient. Scandinavian journal of trauma, resuscitation and emergency medicine. 2012;20:54-54.
4. Enkhbaatar P, Traber Daniel L. Pathophysiology of acute lung injury in combined burn and smoke inhalation injury. Clinical Science. 2004;107(2):137-143.
5. Shirani KZ, Pruitt BAJ, Mason ADJ. The Influence of Inhalation Injury and Pneumonia on Burn Mortality. Annals of Surgery. 1987;205(1):82-87.
6. Ashbaugh D, Boyd Bigelow D, Petty T, Levine B. Acute Respiratory Distress In Adults. The Lancet. 1967;290(7511):319-323.
7. Force* TADT. Acute Respiratory Distress Syndrome: The Berlin Definition. JAMA. 2012;307(23):2526-2533.
8. Matthay MA, Zemans RL. The acute respiratory distress syndrome: pathogenesis and treatment. Annual review of pathology. 2011;6:147-163.
9. Nash G, Blennerhassett JB, Pontoppidan H. Pulmonary Lesions Associated with Oxygen Therapy and Artificial Ventilation. New England Journal of Medicine. 1967;276(7):368-374.
10. Thille AW, Esteban A, Fernández-Segoviano P, Rodriguez J-M, Aramburu J-A, Vargas-Errázuriz P, et al. Chronology of histological lesions in acute respiratory distress syndrome with diffuse alveolar damage: a prospective cohort study of clinical autopsies. The Lancet Respiratory Medicine. 2013;1(5):395-401.
11. Patel BV, Wilson MR, Takata M. Resolution of acute lung injury and inflammation: a translational mouse model. European Respiratory Journal. 2012;39(5):1162-1170.
12. Voelker MT, Fichtner F, Kasper M, Kamprad M, Sack U, Kaisers UX, et al. Characterization of a double-hit murine model of acute respiratory distress syndrome. Clinical and Experimental Pharmacology and Physiology. 2014;41(10):844-853.
13. McLaughlin RF, Jr., Tyler WS, Canada RO. Subgross Pulmonary Anatomy in Various Mammals and Man. JAMA. 1961;175(8):694-697.
14. Glenny RW, Bernard SL, Luchtel DL, Neradilek B, Polissar NL. The spatial-temporal redistribution of pulmonary blood flow with postnatal growth. Journal of Applied Physiology. 2007;102(3):1281-1288.

15. Brogan TV, Mellema JD, Martin LD, Krueger M, Redding GJ, Glenny RW. Spatial and Temporal Heterogeneity of Regional Pulmonary Blood Flow in Piglets. Pediatric Research. 2007;62(4):434-439.
16. Gushima Y, Ichikado K, Suga M, Okamoto T, Iyonaga K, Sato K, et al. Expression of matrix metalloproteinases in pigs with hyperoxia-induced acute lung injury. European Respiratory Journal. 2001;18(5):827-837.
17. Ballard-Croft C, Sumpter LR, Broaddus R, Alexander J, Wang D, Zwischenberger JB. Ovine Smoke/Burn ARDS Model: A New Ventilator-Controlled Smoke Delivery System. Journal of Surgical Research. 2010;164(1):e155-e162.
18. Barrow RE, Spies M, Barrow LN, Herndon DN. Influence of demographics and inhalation injury on burn mortality in children. Burns. 2004;30(1):72-77.
19. Dancey DR, Hayes J, Gomez M, Schouten D, Fish J, Peters W, et al. ARDS in patients with thermal injury. Intensive Care Medicine. 1999;25(11):1231-1236.
20. Alpard SK, Zwischenberger JB, Tao W, Deyo DJ, Traber DL, Bidani A. New clinically relevant sheep model of severe respiratory failure secondary to combined smoke inhalation/cutaneous flame burn injury. Critical Care Medicine. 2000;28(5):1469-1476.
21. Schmalstieg FC, Keeney SE, Rudloff HE, Palkowetz KH, Cevallos M, Zhou X, et al. Arteriovenous CO2 Removal Improves Survival Compared to High Frequency Percussive and Low Tidal Volume Ventilation in a Smoke/Burn Sheep Acute Respiratory Distress Syndrome Model. Annals of Surgery. 2007;246(3):512-523.
22. Soejima K, Schmalstieg FC, Sakurai H, Traber LD, Traber DL. Pathophysiological analysis of combined burn and smoke inhalation injuries in sheep. American Journal of Physiology-Lung Cellular and Molecular Physiology. 2001;280(6):L1233-L1241.
23. Kitamura Y, Hashimoto S, Mizuta N, Kobayashi A, Kooguchi K, Fujiwara I, et al. Fas/FasL-dependent Apoptosis of Alveolar Cells after Lipopolysaccharide-induced Lung Injury in Mice. American Journal of Respiratory and Critical Care Medicine. 2001;163(3):762-769.
24. Katalan S, Falach R, Rosner A, Goldvaser M, Brosh-Nissimov T, Dvir A, et al. A novel swine model of ricin-induced acute respiratory distress syndrome. Disease Models & Mechanisms. 2017;10(2):173-183.
25. Matute-Bello G, Frevert CW, Martin TR. Animal models of acute lung injury. American journal of physiology Lung cellular and molecular physiology. 2008;295(3):L379-L399.
26. Yilin Z, Yandong N, Faguang J. Role of angiotensin-converting enzyme (ACE) and ACE2 in a rat model of smoke inhalation induced acute respiratory distress syndrome. Burns. 2015;41(7):1468-1477.
27. Wang T, Chen X, Zhang W, Xiang X, Leng C, Jia Q. Roles of macrophage stimulating protein and tyrosine kinase receptor RON in smoke-induced airway inflammation of rats. International journal of clinical and experimental pathology. 2015;8(8):8797-8808.
28. Fan E, Brodie D, Slutsky AS. Acute Respiratory Distress Syndrome: Advances in Diagnosis and Treatment. JAMA. 2018;319(7):698-710.

29. Julien M, Hoeffel JM, Flick MR. Oleic acid lung injury in sheep. Journal of Applied Physiology. 1986;60(2):433-440.
30. Grotjohan HP, Van Der Heijde RMJL, Jansen JRC, Wagenvoort CA, Versprille A. A stable model of respiratory distress by small injections of oleic acid in pigs. Intensive Care Medicine. 1996;22(4):336-344.
31. Lewis JF, Tabor B, Ikegami M, Jobe AH, Joseph M, Absolom D. Lung function and surfactant distribution in saline-lavaged sheep given instilled vs. nebulized surfactant. Journal of Applied Physiology. 1993;74(3):1256-1264.
32. Muellenbach RM, Kredel M, Bernd Z, Johannes A, Kuestermann J, Schuster F, et al. Acute respiratory distress induced by repeated saline lavage provides stable experimental conditions for 24 hours in pigs. Experimental Lung Research. 2009;35(3):222-233.
33. Guo Z-l, Lu G-p, Ren T, Zheng Y-h, Gong J-y, Yu J, et al. Partial liquid ventilation confers protection against acute lung injury induced by endotoxin in juvenile piglets. Respiratory Physiology & Neurobiology. 2009;167(3):221-226.
34. Kabir K, Gelinas J-P, Chen M, Chen D, Zhang D, Luo X, et al. Characterization of a Murine Model of Endotoxin-Induced Acute Lung Injury. Shock. 2002;17(4):300-303.
35. Rosenthal C, Caronia C, Quinn C, Lugo N, Sagy M. A comparison among animal models of acute lung injury. Critical Care Medicine. 1998;26(5):912-916.
36. Belenkiy S, Ivey KM, Batchinsky AI, Langer T, Necsoiu C, Baker W, et al. Noninvasive Carbon Dioxide Monitoring in a Porcine Model of Acute Lung Injury Due to Smoke Inhalation and Burns. Shock. 2013;39(6):495-500.
37. Yousuf T, Brinton T, Murtaza G, Wozniczka D, Ahmad K, Iskandar J, et al. Establishing a gradient between partial pressure of arterial carbon dioxide and end-tidal carbon dioxide in patients with acute respiratory distress syndrome. Journal of Investigative Medicine. 2017;65(2):338-341.

Figures

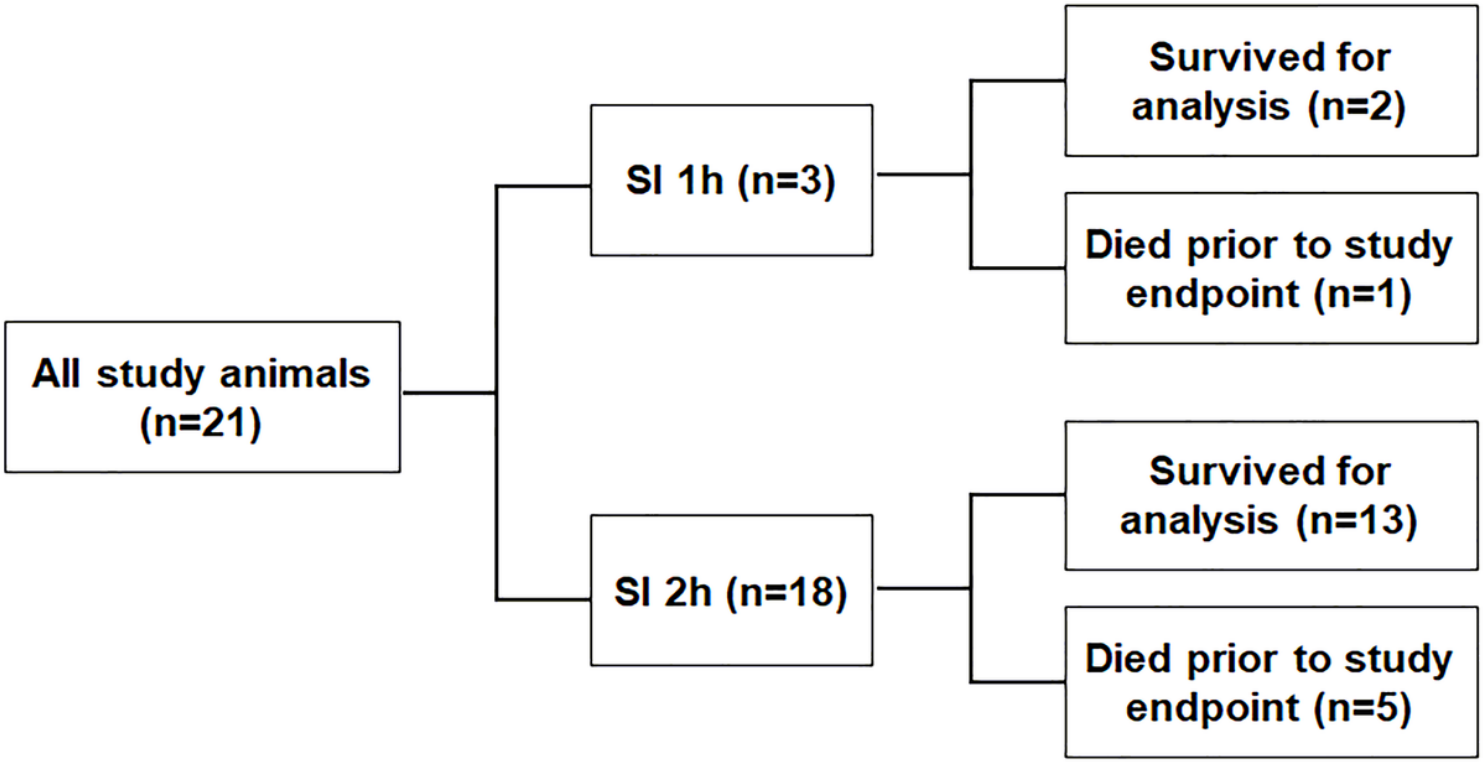

Figure 1

Schematic diagram of the smoke generator system and delivery circuit.

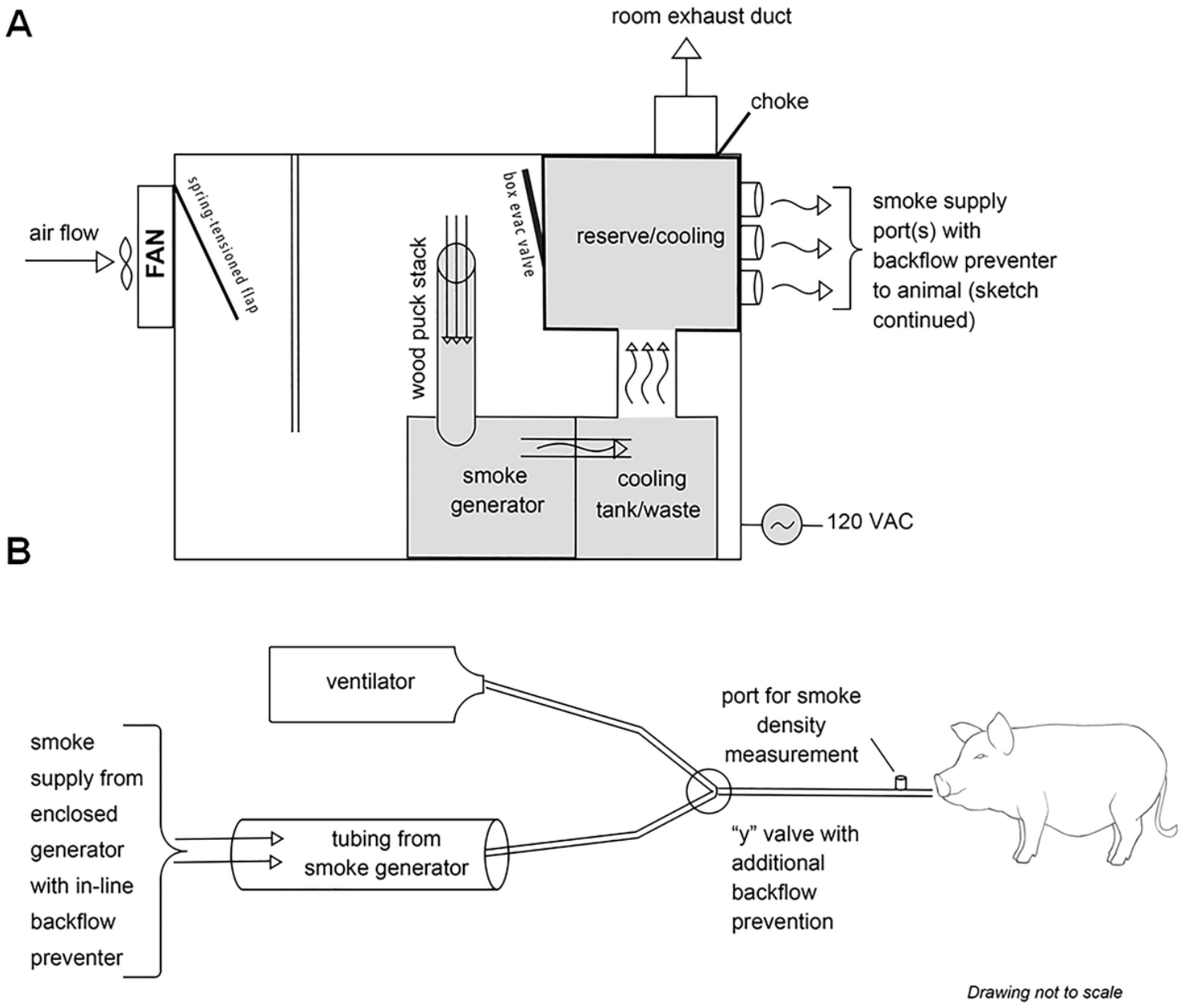

Figure 2

Flow diagram representing animals assigned to different study groups.

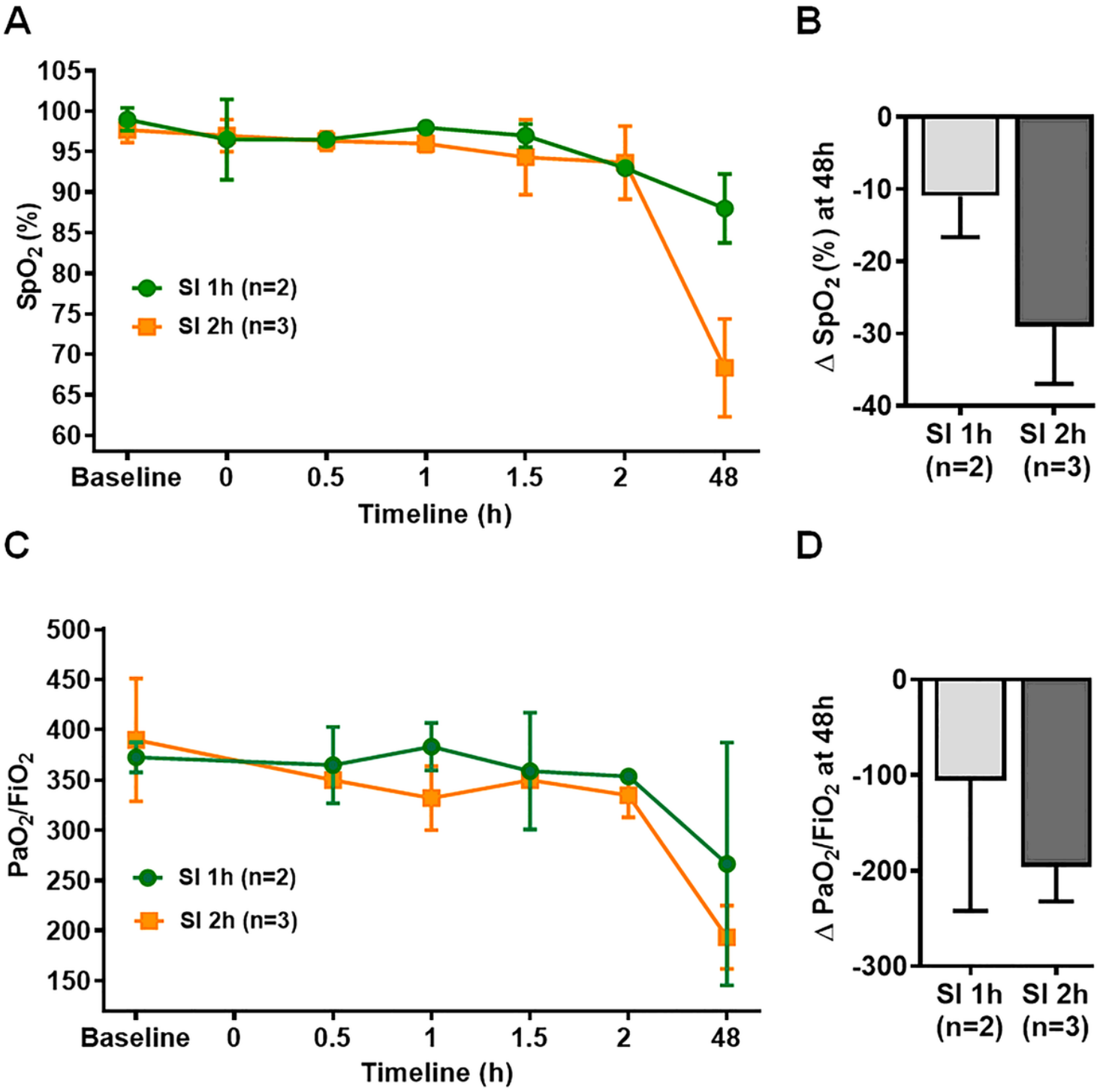

Figure 3

Effect of smoke duration in large animal. A and B, Peripheral oxygen saturation (SpO2) level was measured in 1h- and 2h-smoke inhalation groups designated as “SI 1h” and “SI 2h”, respectively, at different time points from 0h to 48h (A). Statistical analysis of the delta SpO2 (designated as SpO2) between SI 1h and SI 2h groups (B). SpO2 for each group represented the difference in SpO2 level between baseline and 48h post smoke exposure. C and D, The ratio of partial pressure of arterial oxygen (PaO2) and fraction of inspired oxygen (FiO2), designated as “PaO2/ FiO2” was measured in SI 1h and SI 2h group of animals (C). Statistical analysis of the delta PaO2/FiO2 (designated as PaO2/FiO2)

between SI 1h and SI 2h groups (D). ΔPaO2/FiO2 for each group represented the difference in PaO2/FiO2 level between baseline and 48h post smoke exposure. A p value of < 0.05 was considered statistically significant.

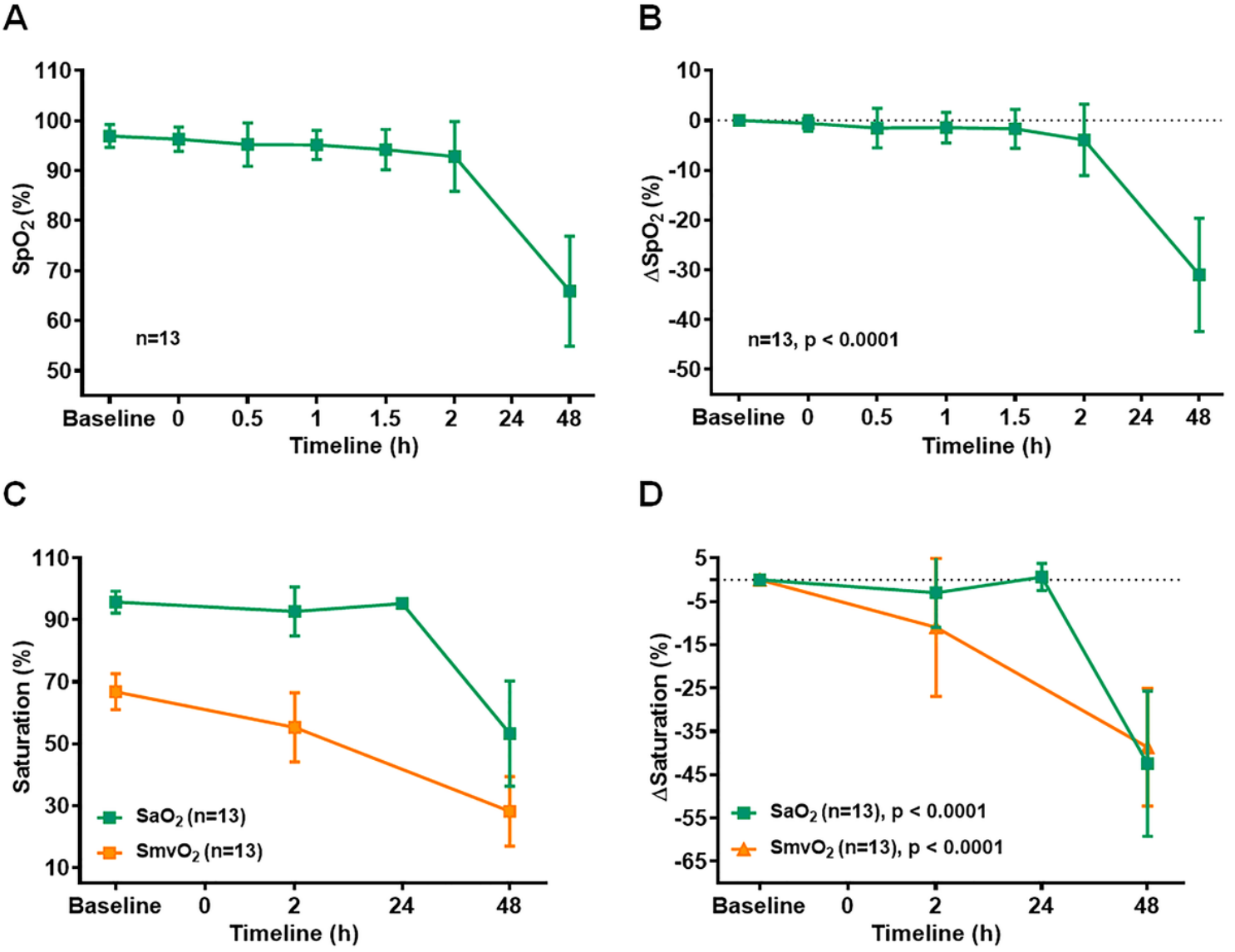

Figure 4

Smoke inhalation reduced oxygen saturation in large animals. A and B, Peripheral oxygen saturation (SpO2) level was measured in a different set of 2h smoke inhalation group designated as “SI” at different time points from 0h to 48h (A). ΔSpO2 values between baseline and different time points (B). C and D, Arterial oxygen saturation (SaO2) and mixed venous oxygen saturation (SmvO2) levels were measured in SI group at baseline, 2h, 24h, and 48h time points (C). Delta SaO2 (ΔSaO2) and delta SmvO2 (ΔSmvO2) values were calculated between baseline and different time points (D). Delta value for each parameter represented the difference with corresponding baseline values. SaO2 level was measured at 24h for n = 8, SpO2 and SmvO2 levels were not measured at 24h time line. A p value of < 0.05 was considered statistically significant.

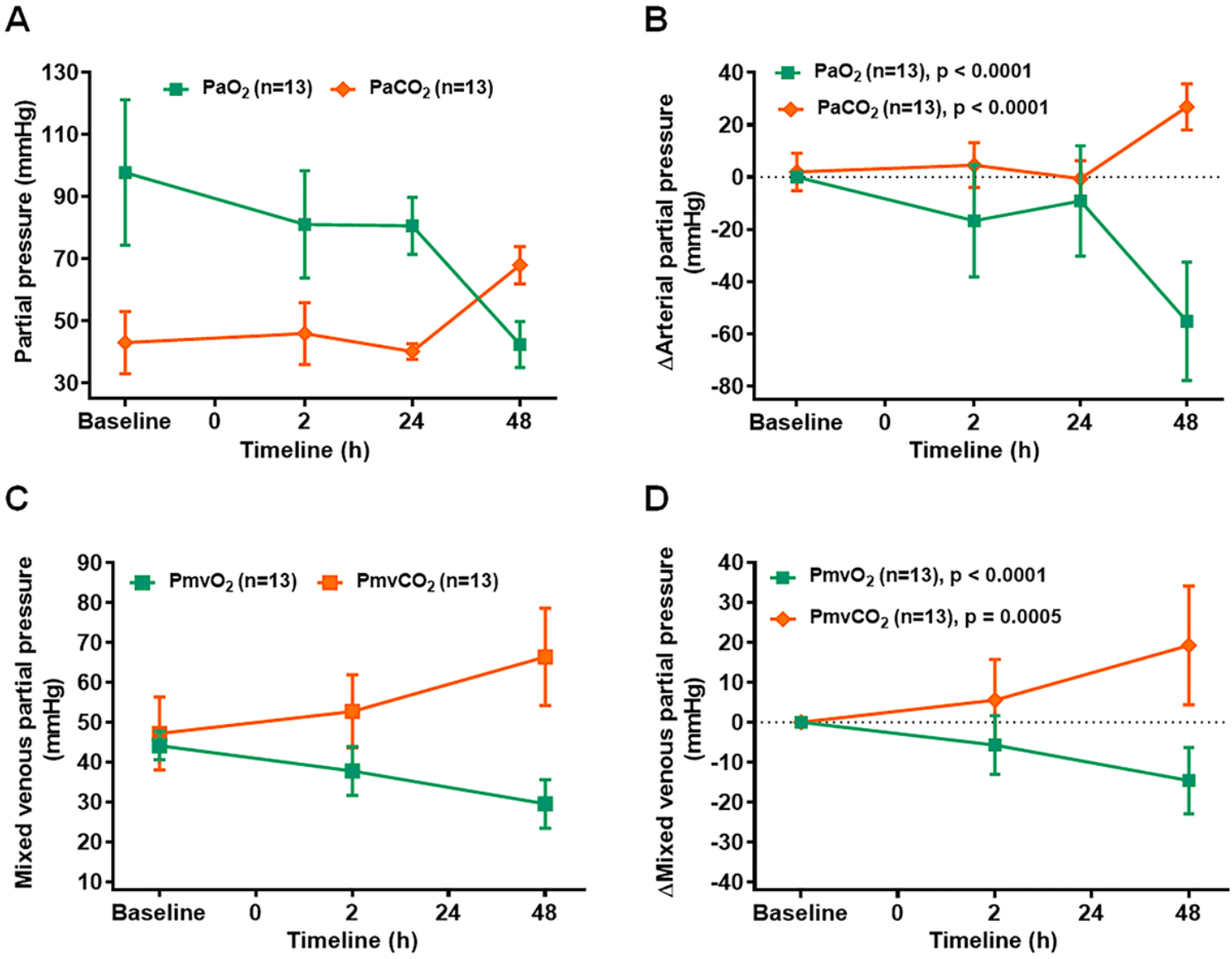

Figure 5

Smoke inhalation reduces PO2 with reciprocal increase in PCO2. A and B, Arterial partial pressure of oxygen (PaO2) and carbon-dioxide (PaCO2) levels were measured in SI group at baseline, 2h, 24h, and 48h time points (A). Delta PaO2 (ΔPaO2) and delta PaCO2 (ΔPaCO2) values between baseline and different time points (B). C and D, Mixed venous partial pressure of pressure of oxygen (PmvO2) and carbon dioxide (PmvCO2) level were measured in SI group at baseline, 2h, 24h, and 48h time points (C). Delta PmvO2 (ΔPmvO2) and delta PmvCO2 (ΔPmvCO2) values were calculated between baseline and different time points (D). Delta value for each parameter represented the difference with corresponding baseline values. PaO2 and PaCO2 levels were measured at 24h for n = 8; PmvO2 and PmvCO2 levels were not measured at 24h time line. A p value of < 0.05 was considered statistically significant.

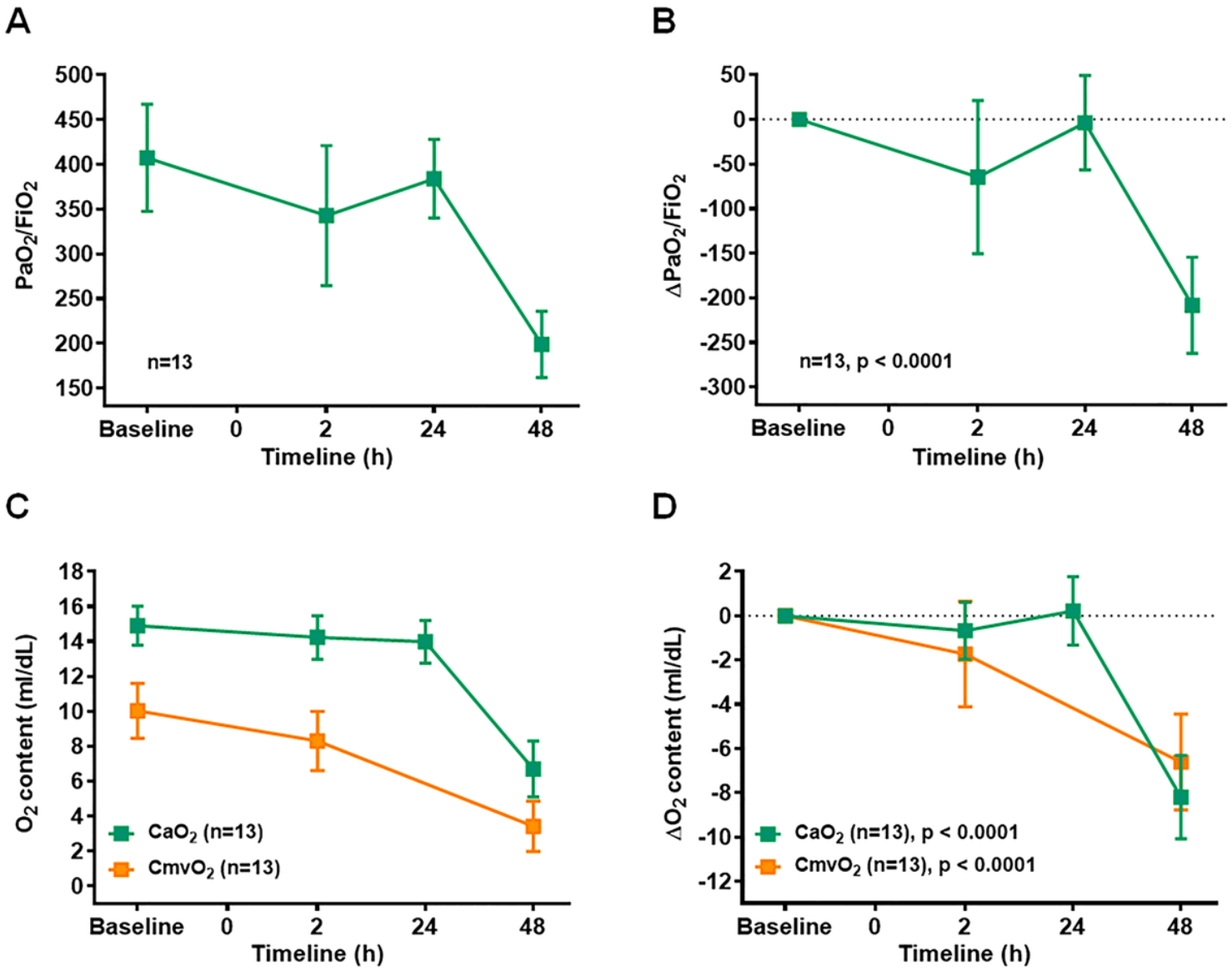

Figure 6

PaO2/FiO2 and total oxygen content reduced in smoke inhalation induced lung injury. A, The ratio of PaO2 and FiO2, designated as “PaO2/FiO2” was measured in SI group of animals at baseline, 2h, 24h, and 48h time points. B, Delta PaO2/ FiO2 (PaO2/FiO2) values were calculated between baseline and different time points. C, Total arterial oxygen content (CaO2) and total mixed venous oxygen content (CmvO2) levels were measured in SI group at baseline, 2h, 24h and 48h time points. D, Delta CaO2 (CaO2) and delta CmvO2 (CmvO2) values were calculated between baseline and different time points (D). Delta value for each parameter represented the difference with the corresponding baseline values. PaO2/FiO2 and CaO2 and levels were measured at 24h for n = 8 and n = 6 respectively; CmvO2 level was not measured at 24h time line. A p value of < 0.05 was considered statistically significant.

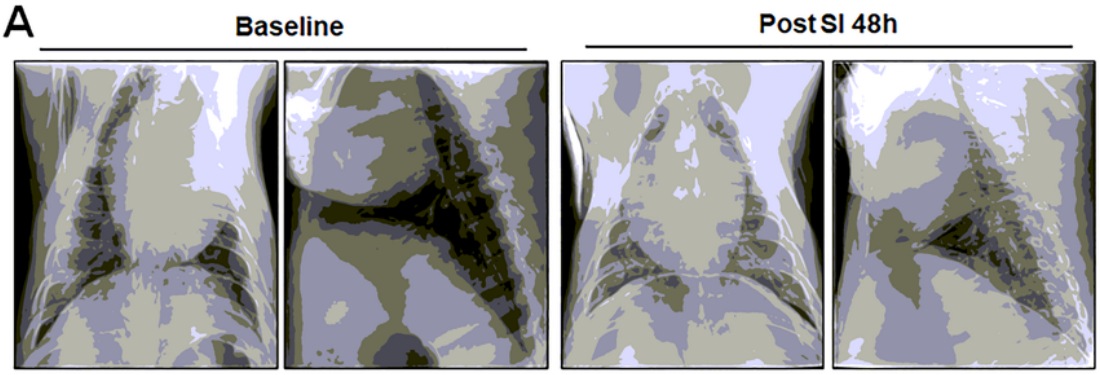

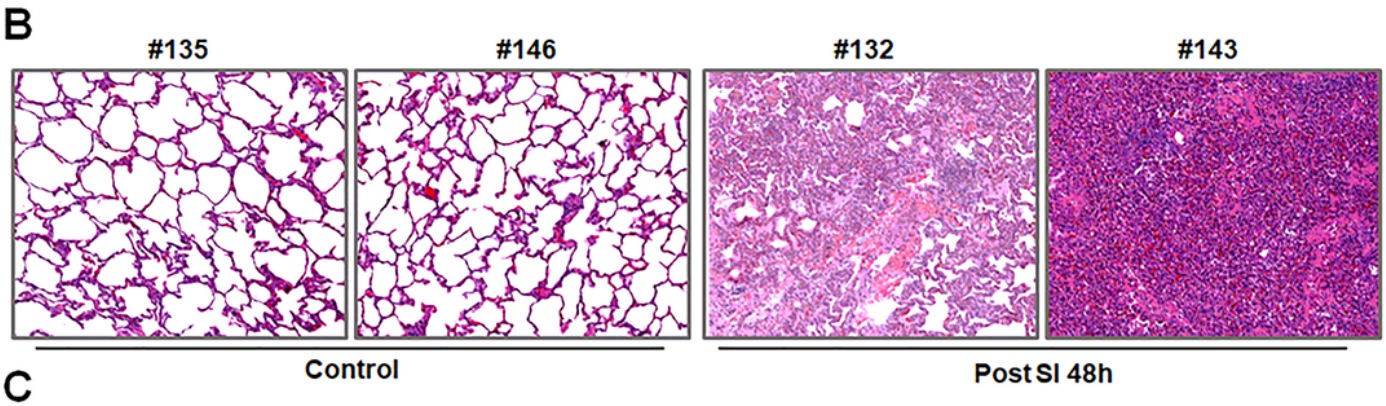

C

Lung injury score

Parameters	Leucocyte infiltration	Intra-alveolar hemorrhage	Alveolar edema
Control (n=2)	1.77±0.5	0	0
Post SI 48h (n=5)	2.43±0.3	0.62±0.58	0.15±19

Values are mean ± SD

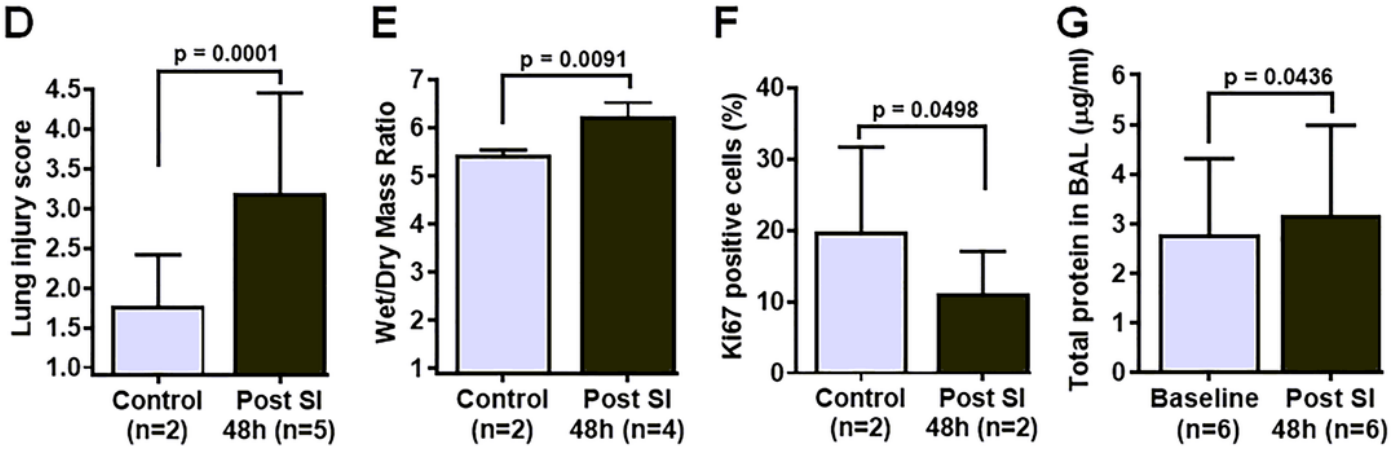

Figure 7

Effect of smoke inhalation in lung parenchyma. A, Ventral-dorsal and lateral view chest x-rays at baseline and 48h after smoke inhalation. B, C, and D, Hematoxylin and eosin (H&E) staining on two sets of paraffin embedded lung tissue sections of control and SI animals (B). Statistical analysis of lung injury score between control and SI animals (C, D). E, Statistical analysis of wet/dry weight (W/D) ratio between control and SI animals. F, Percentage of Ki67 positive cells on the paraffin embedded lung tissue sections

of control and SI animals. G, Quantification of total protein concentration of BAL fluid samples in SI group at baseline and 48h post smoke inhalation. A p value of < 0.05 was considered statistically significant.

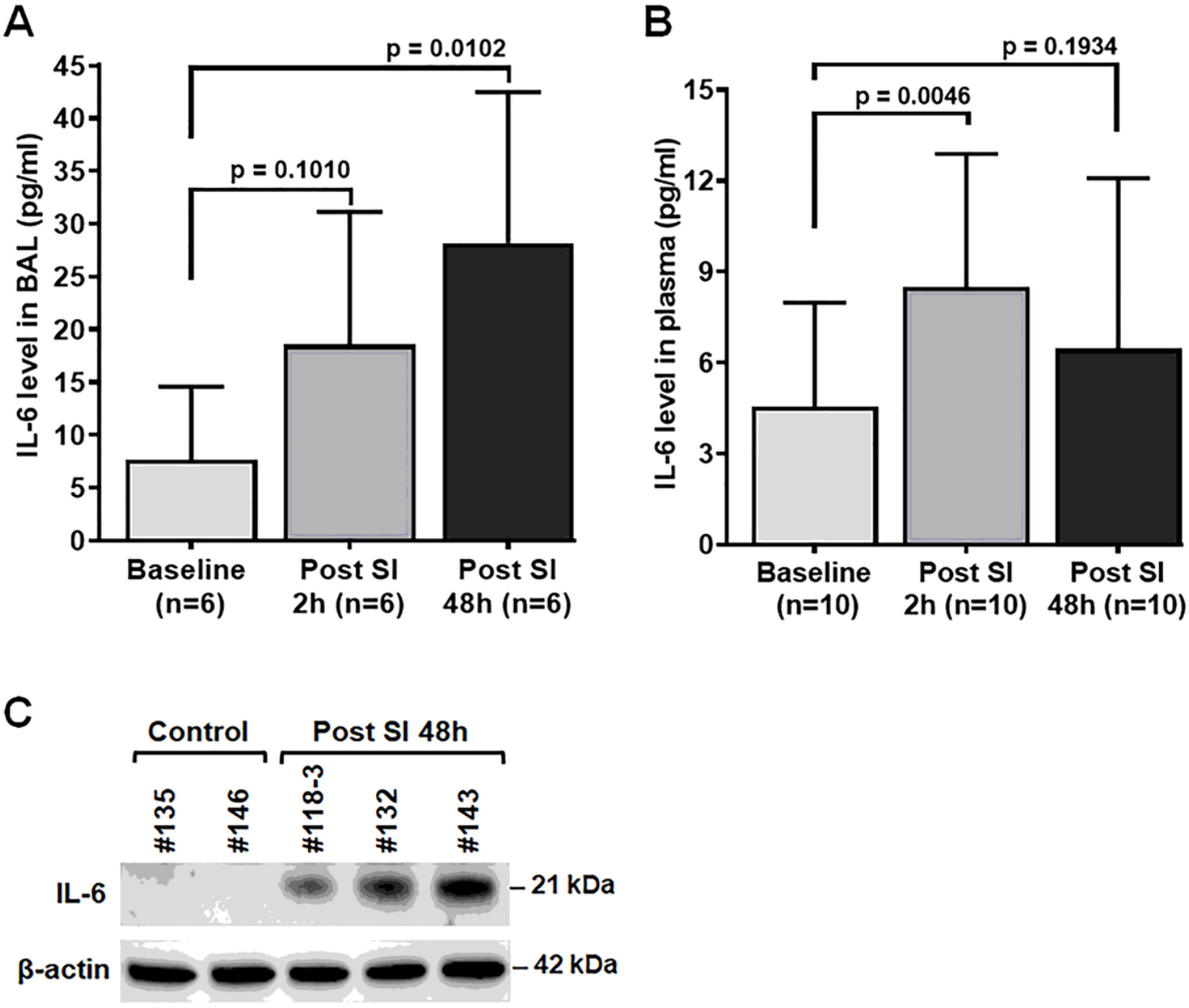

Figure 8

Effect of smoke inhalation on IL-6 expression. A, IL-6 expression level in plasma samples of SI animals at baseline, 2h and 48h time points. B, IL-6 expression level in BAL fluid samples of SI animals at baseline, 2h and 48h time points. C, Immunoblot analysis of IL-6 expression level in fresh frozen lung tissues of SI and control animals. A p value of < 0.05 was considered statistically significant.